Journal of Renewable Energy and Sustainable Development (RESD) Volume 10, Issue 2, December 2024 - ISSN 2356-8569
http://dx.doi.org/10.21622/RESD.2024.10.2.1054

Received on, 10 October 2024 Accepted on, 06 November 2024 Published on, 20 November 2024

Experimental and Computational Analysis of Air Injection as a Mitigation Technique for Silt Erosion in Hydro Turbines

Prashant Dhiman [1], Varun Pratap Singh [2], and Ashish Karn [3]

[1,2,3] Multi phase flow Laboratory, Mechanical Cluster, School of Advanced Engineering, UPES, Dehradun, Uttarakhand, India

[2] Solar Thermal Energy Research Group, Department of Mechanical and Mechatronics Engineering, Stellenbosch University, Stellenbosch, 7600, South Africa

500099827@stu.upes.ac.in, varunpratap.singh@ddn.upes.ac.in, akarn@upes.ac.in

ABSTRACT

Hydroelectric power plants, essential to renewable energy generation, face persistent challenges of silt and cavitation erosion, particularly pronounced in the sediment-rich Himalayan region. Sediment-laden water accelerates erosion in critical components, including turbine blades and guide vanes, diminishing efficiency and operational lifespan. This study introduces an innovative air injection technique designed to reduce silt erosion on guide vane surfaces. Both computational simulations and experimental testing, utilizing a custom-built rotating disc apparatus, were conducted to assess the efficacy of this approach. Erosion tests were performed on guide vanes with and without air injection, using NACA 4412 hydrofoil profiles set at a 10° angle of attack. Key parameters included air injection velocities ranging from 7.5 m/s to 17.5 m/s, a silt concentration of 2500 ppm, and air injection angles set at 90°. The study measured erosion rates, material loss, and surface erosion patterns. Simulation outcomes demonstrated a 40% reduction in erosion, while experimental findings revealed efficiency gains of 27% to 38%, with optimal results at an air injection velocity of 12.5 m/s. The novelty of this technique lies in its creation of a protective air buffer on the vane surface, which mitigates direct silt impact, significantly reducing erosion. This method offers a compelling advancement over traditional mitigation strategies such as material coatings and sediment chambers.

Index-words: *Hydro turbines, Hydrofoil, Silt erosion, Air-injection, Guide vanes, Erosion mitigation.*

Nomenclature:

Symbol	Definition with unit	Greek Symbol	Definition
a	Angle of attack of hydrofoil (in degrees)	μ	Dynamic viscosity of water
d	Angle of air injection (in degrees)	ν	Kinematic viscosity of water
m	Sediment concentration in the water stream (in ppm)	ρ	Density of water stream
U_∞	Free water stream velocity (in m/s)	**Dimensionless Parameters**	**Definition**
v	Air injection velocity (in m/s for simulations)		
c	Chord length of guide vane (in m)	C_d	Coefficient of drag
Abbreviation	**Definition**		
AR	Aspect ratio of leading edge of guide vane		
HVFS	High-Velocity Flame Spraying		
HVOF	High-Velocity Oxygen Fuel	Re	Reynolds Number
NACA	National Advisory Committee for Aeronautics		
RDA	Rotary Disc Apparatus		
SMAW	Shielded Metal Arc Welding		
SST	Shear Stress Transport		

Volume 10, Issue 2, December 2024 - ISSN 2356-8569
http://dx.doi.org/10.21622/RESD.2024.10.2.1054

I. INTRODUCTION

Hydroelectric power offers a highly efficient and reliable solution for energy production, with the potential to maximize power generation at relatively low operational costs. As the leading source of renewable energy, hydropower meets approximately 19% of the global energy demand. Beyond energy production, hydroelectric plants serve multiple purposes, including irrigation, flood control, and supporting regional economic activities such as tourism and local transportation. These ancillary benefits contribute to economic growth in the areas surrounding hydroelectric facilities [1].

Despite these advantages, hydropower plants face several operational challenges that disrupt their efficiency and increase maintenance needs. Among the key issues identified across various turbine types are cavitation, erosion, fatigue, and material defects [2]. Silt erosion is particularly prevalent in hydropower plants situated along sediment-laden rivers, such as those in the Himalayan regions of India. The high concentration of silt in these water streams accelerates the degradation of essential components like nozzles, guide vanes, and runner blades as shown in Figure 1, leading to increased downtime and higher maintenance costs [3].

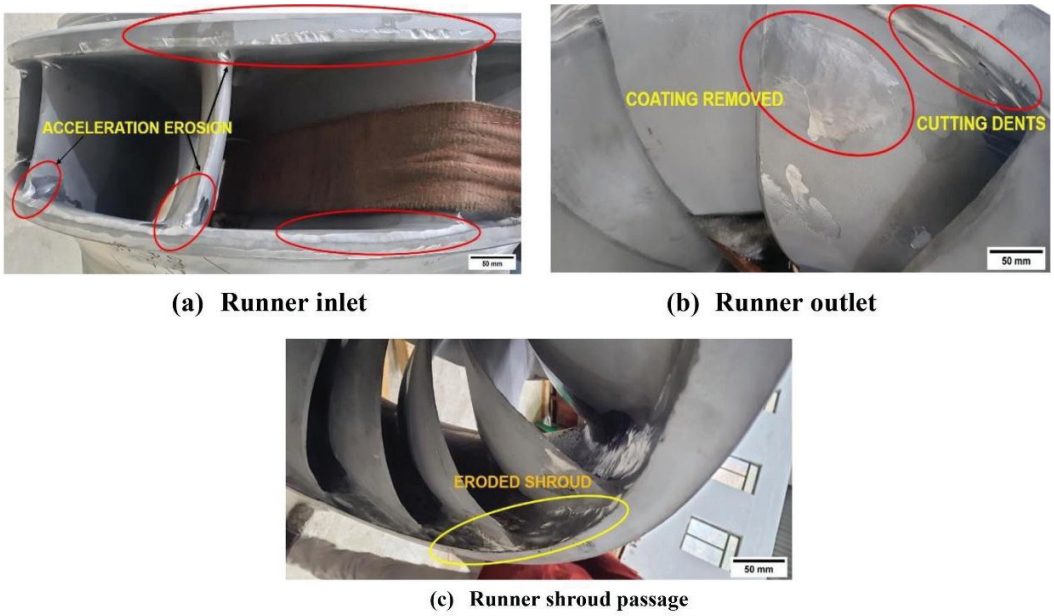


Fig. 1. Silt erosion at various positions of runner: (a) Runner inlet (b) Runner outlet and (c) Runner shroud passage. Image adapted from Sharma & Gandhi [4]

Silt erosion, also referred to as abrasive erosion, occurs when the surface material of turbine components is progressively worn down by the continuous impact of silt particles under continuous shear action [5]. Studies highlight sediment management as a key strategy in mitigating silt erosion, primarily through the construction of de-silting chambers or sediment basins, which allow silt particles to settle before the water enters the turbines [6], [7], [8]. Real-time monitoring systems play a crucial role in managing silt concentrations by providing data that enables operators to take corrective actions when sediment parameters, such as size and shape, exceed specified limits. These systems function as early warning mechanisms, allowing plants to adjust operations accordingly. Sediment chambers and monitoring systems can reduce the impact of silt, but they are not sufficient to fully eradicate silt erosion [9], [10], [11], [12].

Recent research suggests that applying protective coatings to turbine components could further minimize erosion, although the technique of coating is still being refined through ongoing studies. In the phenomenon of coating, the microstructure of the developed coatings plays a crucial role in determining their effectiveness in resisting silt erosion. Researchers have explored various techniques to enhance the microstructure of coatings applied to turbine substrate materials, concluding that methods such as High-Velocity Oxygen Fuel (HVOF) spraying and plasma spraying offer superior resistance to silt erosion [13]. Numerous studies have identified CA6NM

Volume 10, Issue 2, December 2024 - ISSN 2356-8569
http://dx.doi.org/10.21622/RESD.2024.10.2.1054

(martensitic stainless steel with 0.06% of Carbon) as a commonly used substrate material in hydro turbines, owing to its favorable properties [14], [15], [16]. CA6NM is often combined with a variety of coating materials, including Ni (Nickel), Cr (Chromium), Stellite-6 (wear resistant alloy containing cobalt, chromium, tungsten, molybdenum and carbon), Cr_2O_3 (Chromium (III) oxide, one of the principal oxides of chromium), Ni-Al_2O_3 (Nickel containing Aluminum Oxide or Nickel Aluminate, the presence of Ni increases the fracture toughness and thermal properties of Aluminum oxide), Ni-xTiO_2 (Nickel doped Titanium dioxide), Ni-xAl_2O_3 ((Nickel Aluminate or Nickel present in variable composition of Aluminum oxide), among others, to enhance its resistance to erosion[17], [18], [19], [20]. Substrate-coating combinations may be applied using several coating techniques, particularly Oxygen Fuel Process (OFP), High-Velocity Oxygen Fuel (HVOF), Shielded Metal Arc Welding (SMAW), High-Velocity Flame Spraying (HVFS), Plasma sprayed, Microwave clad, and other processes [21], [22], [23], [24], [25]. Significant research to increase the life and the performance of hydro turbines might be done by investigating the best combinations of substrate materials, coatings, and application processes. This comprehensive method of combining different coating techniques with different coating materials shows potential for increasing the operating life of hydro turbines. After exhaustive numerical, experimental, and case studies, Padhy and Saini [26] emphasized that it is impossible to completely remove the silt erosion. However, existing literature indicates that silt erosion can be significantly reduced by implementing appropriate design parameters, alongside desilting chambers, and coating technologies.

One of the potential alternative technologies may involve modified turbine blades or guide vanes that incorporate air injections. While air injection in hydro turbines is a well-known phenomenon, its previously applications have been primarily focused on increasing dissolved oxygen levels [27], [28], [29], [30] and reducing vortex formation in draft tubes within hydropower plants [31], [32], recent studies suggest the effect of air injection in mitigating cavitation, though these are focused on water tunnel experiments and cavitation alone [33], [34], [35]. Also, a preliminary study conducted by Dhiman et al. [36] reports the effect of air injection in mitigating silt erosion in hydro turbines, which support the hypothesis. Also, numerical studies in mitigating silt erosion with the help of air injection are reported and various other cases of air injection are discussed in the studies [37]. While conventional methods like sediment management and surface coatings provide some relief from silt erosion in hydro turbines, they fail to fully mitigate the continuous abrasive impact of sediment-laden water, particularly in high-silt regions like the Himalayan rivers. Furthermore, limited research has explored alternative strategies, such as air injection, beyond surface modifications. Previous studies focus on air injection for cavitation control, but its potential for reducing silt erosion is not fully investigated, particularly through comprehensive computational and experimental analysis.

The objective of this study is to introduce and validate a novel air injection technique as a means to mitigate silt erosion in hydro turbines. By creating a protective air layer over guide vanes, the study aims to reduce the direct impact of silt particles, thus enhancing turbine durability and minimizing maintenance requirements. The effectiveness of this technique is evaluated through both computational simulations and experimental testing, providing a robust framework for its potential real-world application.

The structure of this paper is as follows: Section 2 details the methodology, including the computational setup and experimental procedures. Section 3 presents the results and discussion, offering a comprehensive dataset on the effectiveness of the air injection technique for mitigating silt erosion. Finally, Section 4 concludes by summarizing the findings, emphasizing percentage reductions in erosion as a measure of the technique effectiveness.

II. METHODOLOGY

In this study, the NACA 4412 hydrofoil profile is selected for the guide vanes to investigate silt erosion behavior. The research approach involves two stages: first, numerical simulations are conducted to assess erosion rates and flow patterns, followed by experimental validation using a specially designed erosion testing setup known as the rotary disc apparatus. Sediment samples are collected from both the upstream and downstream of the Maneri Bhali dam and sieved to a particle size of 200 μm to meet the experimental requirements. The erosion patterns on the guide vane samples are analyzed through a comparative study of before and after images, allowing for precise observation of material loss. The recorded material loss is used to calculate the erosion rate and evaluate the

effectiveness of the proposed air injection technique in mitigating silt erosion. Finally, conclusions are drawn based on both the numerical simulations and experimental data, and recommendations are made for the potential application of this technique to improve the durability of hydro turbines operating in silt-laden environments[38].

A. Computational Study

1. Computational Setup

ANSYS Fluent 19.1 commercial package software is used in this computational study and is applied to examine and anticipate the erosion behavior of the ventilated guide vanes in Francis turbine in the silt-laden water stream in which primary, secondary, and discrete phases are represented for the dynamic momentum exchange among water, air, and sediment particles. This study focuses on the interaction of physical fluid dynamics through a three-phase system including fluid-solid, fluid-fluid, and solid-solid to understand and evaluate the interaction of sediment particles present in a water stream on a hydrofoil profile NACA 4412 of an aerated guide vane. The Eulerian approach enables the interaction between water (silt-laden water) and air once the numerical solution has commenced, stabilizing the resulting flow field. It is anticipated that the relationship between Reynolds number (*Re*) and coefficient of drag (C_d) will be non-linear when *Re* exceeds unity (where, $Re = \rho UL/\mu$ and $C_D = F_D/0.5\rho U^2 A$; ρ,μ,L,A,U and F_D denote the fluid density, viscosity, length scale, area , fluid velocity and drag force, respectively). The accurate selection of drag and turbulence models is essential for resolving the target flow components effectively. In this study, the Schiller-Naumann dynamic drag model is employed to facilitate accurate momentum exchange within fluid mixtures. Prior research by Silva (2015) demonstrated that the Schiller-Naumann model aligns more closely with experimental data compared to the Gidaspow model [39].

The Euler-Euler-Lagrange model combined with the *K*-omega SST turbulence scheme. The element counts for O-Grid Hexahedral mesh are 0.949, 1.276, and 1.401 million for cases 1, 2, and 3, respectively. The element counts for Cartesian Cut Cell mesh are 0.51, 1.04, and 1.241 million for cases 4, 5, and 6, respectively, along with the values of coefficient of drag are shown in Table I. The current study focuses on the different system variables and the test parameters presented in Table II, including sediment load in the flowing water stream (*m*) is 2500 ppm, air injection velocity (*v*) ranging from 7.5 m/s to 17.5 m/s, air injection angle (*d*) about 90, the angle of attack (*a*) for the guide vanes is 10° and the free stream velocity of water (U_∞) is 10 m/s.

TABLE I
DESCRIPTION OF ELEMENT COUNTS (IN MILLIONS) AND COEFFICIENT OF DRAG FOR DIFFERENT MESH TYPES AND THEIR DIFFERENT CASES.

Mesh type		Element Count (million)	Coefficient of Drag (C_d)
O-Grid Hexahedral Cell	Case-1	0.949	0.696
	Case-2	1.276	0.674
	Case-3	1.401	0.651
Cartesian Cut Cell	Case-4	0.51	0.716
	Case-5	1.04	0.648
	Case-6	1.241	0.644

2. Simulation Domain and Constraint Parameters

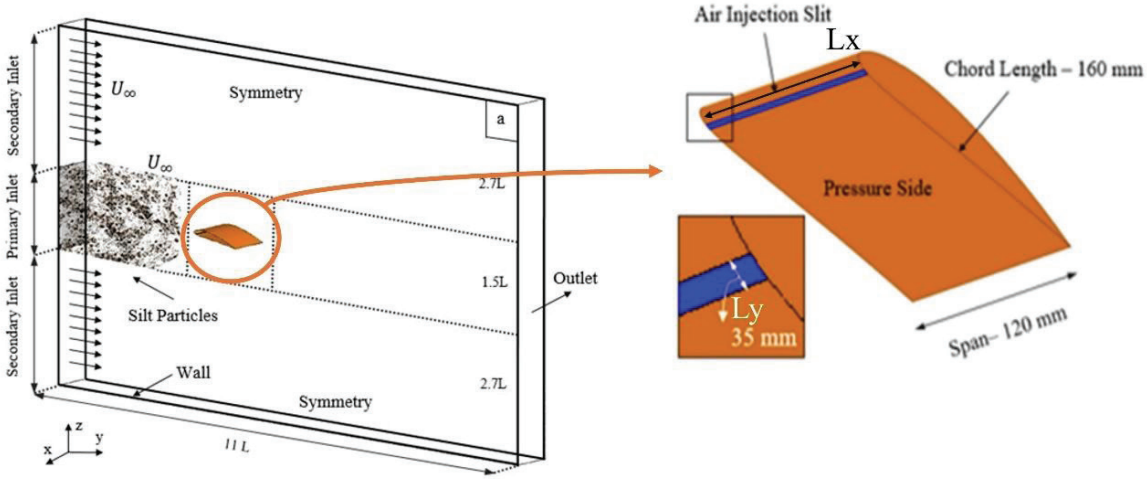
The structural characteristics of the physical model considered for a computational study that provides the erosion rates of the guide vanes exposed to the sediment-suspended water stream are presented in Figure 2 (a). The fluid flow path is subsequently divided into main and auxiliary inlets to enhance control, allowing for a focused injection of particles directly along the hydrofoil's path. The dimensions of the computational domain are 1.76 m in the direction of the stream (along the Y-axis), 0.12 m in the direction of the guide vane span (along the X-axis), and height-wise, it is 1.06 m (along the Z-axis). Sediment particles are allowed to emit exclusively from the primary zone, covering an area of 0.052 m². Meanwhile, the water stream flows into the system at a velocity (U_∞) of 10 m/s across all sections, with turbulence intensity maintained below 0.05%.

Zhang et al. [40] previously indicate that the projection of erosion becomes unaffected by the concentration of particles beyond a certain extent, a finding later confirmed by Vieira et al. [41] in their numerical analysis of particles of erosion in internal pipes. Likewise, Mansouri et al. [42] conduct a jet impingement study with 50,000 particles for both gas-solid and liquid-solid scenarios, concluding that erosion outcomes are not influenced by the number of particles. The statistical correlation applies to the current study, where 12,900 incoming particles

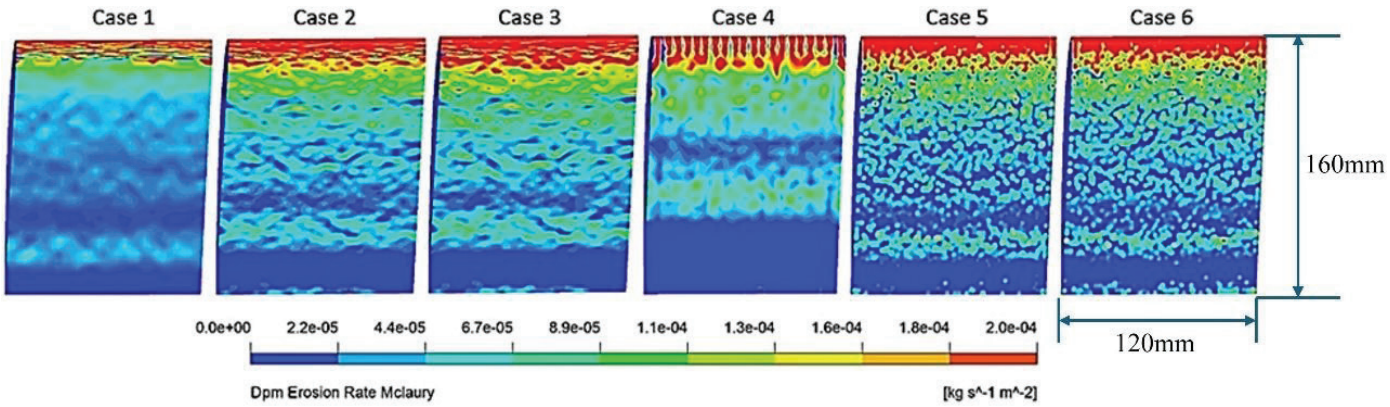
Volume 10, Issue 2, December 2024 - ISSN 2356-8569
http://dx.doi.org/10.21622/RESD.2024.10.2.1054

per cycle are found to be sufficient, with one cycle equating to ten iterations. This is achieved using the Rosin-Ramler technique, which involves a discrete injection cycle across various particle sizes, ensuring a 100% mass fraction for each size range. The study uses input constraints of particle sizes with a minimum of 0.08 mm, a maximum of 0.2 mm, and an average of 0.1 mm to align closely with sieve test data obtained from sediment samples collected from three distinct hydropower plant locations, each weighing around 1 kg and exhibiting varying grain sizes. Most sediment particles are within the grain size range of 0.15 mm.

The silt laden water stream impacts the guide vane of profile NACA 4412 hydrofoil, with a chord length (acting as baseline) of 0.16 meters (denoted as $c = L$). Reynolds number (Re_L) of 1.22×10^6 based on L, is fixed for all experiments where the Reynolds number is defined as $Re_y = \rho U_\infty y / \mu$, with ρ and μ representing the water density and dynamic viscosity, respectively. To assess the erosion rate with aeration, a continuous slit for air injection is considered at $y=L/8$ from the leading edge having an aspect ratio (AR) of 3.42 ($AR = L_x/L_y$), here aspect ratio is defined as the ratio of the length of the slit to the width of the slit which are represented as L_x and L_y. Also, this ratio is considered as it influences the volume of air that can be injected and affects the flow characteristics and dispersion of the injected air. This specific injection design is chosen to adhere to the Coanda effect, allowing the air to create a protective layer on the pressure side of the blade. This setup aims to alter particle trajectories and reduce the overall erosion effect, which occurs during impact interactions.



(a)



(b)

Fig. 2. (a) Computational domain and Physical model considered in the computational study (b) Results from the grid refinement tests were conducted to evaluate the erosion behavior on the pressure side of a hydrofoil, utilizing two types of mesh: O-grid hexa (Cases 1-3) and Cartesian cut cell (Cases 4-6)

3. Validation

The conformity of the computational method is validated by analyzing grid sensitivity (See Table I and Figure 2 (b)) and later by experimental analysis. For this evaluation, high-order grids are created using Cartesian cut-cell and O-grid hexahedral cell types[43],[44],[45]. Spherical particles are considered along with other certain assumptions like particles are independent of each other, particle splitting is not allowed, rotation of particles is ignored, and pitting on the hydrofoil is not accounted. These assumptions are designed to optimize the conditions for particle-wall interactions. Solid particle velocity is evaluated by using Newton's kinetic equation within the Discrete Particle Model and the particle momentum equation in the Fluid Flow Model. Furthermore, the erosion model incorporates the characteristics of the wall material, considering that the material is ductile. This approach provides a clear structure, starting with the validation of the computational method and then detailing the simulation configuration and corresponding conditions. In the present study SST Model is used for simulation of an accurate estimation of drag caused by viscous effects normal to the hydrofoil wall which depends on how effectively the boundary layer is resolved, which correlates directly with the degree of mesh refinement. To achieve this using the K-omega model for low Reynolds number flows, it is crucial to ensure a dimensionless distance, y^+ of 5 or lower, indicating the boundary between the viscous sublayer and buffer layer. In this context, y^+ is defined as: $y^+ = y.\ u_\tau / \nu$, where y represents the height of the first cell, u_τ denotes the frictional velocity, and ν is the kinematic viscosity. In the current case, 24 inflation layers are chosen, with a 12% growth rate between successive layers and a bias factor of 36, to keep y^+ below 5 for both cut-cell and O-grid mesh types. A pressure-based solver is employed to solve the governing equations over control volumes to achieve a steady-state solution. A sophisticated coupled algorithm is utilized to solve all variables with pressure interpolation, rather than simpler methods, to ensure accuracy and achieve an accelerated convergence error threshold of 10^{-6}. A second-order upwind scheme is used to discretize the nonlinear convective terms in the momentum equations, followed by the viscous terms.

B. Experimental Setup

To investigate the effectiveness of the air injection technique in mitigating silt erosion on guide vanes, a comprehensive experimental setup is designed. This setup consists of a specially constructed rotary disc apparatus (RDA), which simulates the conditions experienced by guide vanes in a sediment-laden water stream. The RDA allows for controlled testing of material samples under varying conditions of silt concentration and flow velocity. The guide vane specimens, based on the NACA 4412 hydrofoil profile, are subjected to silt-laden water to measure erosion rates and analyze material degradation patterns. Additionally, sediment samples are carefully collected from the upstream and downstream sections of the Maneri Bhali dam and are sieved to a consistent particle size of 200 μm for uniformity in experimentation. This experimental procedure enables a detailed examination of the erosion patterns and provides a platform for evaluating the mitigation potential of air injection on turbine components.

1. The Test Rig: Rotating Disk Rotating Apparatus

On-site investigations to assess silt erosion in hydro turbines pose substantial challenges due to the remote locations of erosion sites, coupled with high costs, extended time requirements, and logistical complexities. Advanced tools and sensors capable of providing precise quantitative data offer a practical alternative for thorough analysis. These sophisticated instruments enable accurate data collection and facilitate detailed examination, essential for gaining insight into erosion mechanisms and addressing core issues. Although deploying such equipment can be resource-intensive, it is often essential to obtain the high-quality data required for rigorous scientific inquiry [46]. A laboratory setting provides a controlled environment for investigating erosion patterns, allowing researchers to develop effective erosion mitigation techniques and deepen their understanding of underlying processes. Prior studies demonstrate the feasibility of formulating erosion rate correlations through simplified experimental setups, such as jet rigs [47] or pot testers [48], which allow for intentional modifications of substrate material and sediment characteristics, as well as variations in geometric and flow parameters like impingement angle and velocity.

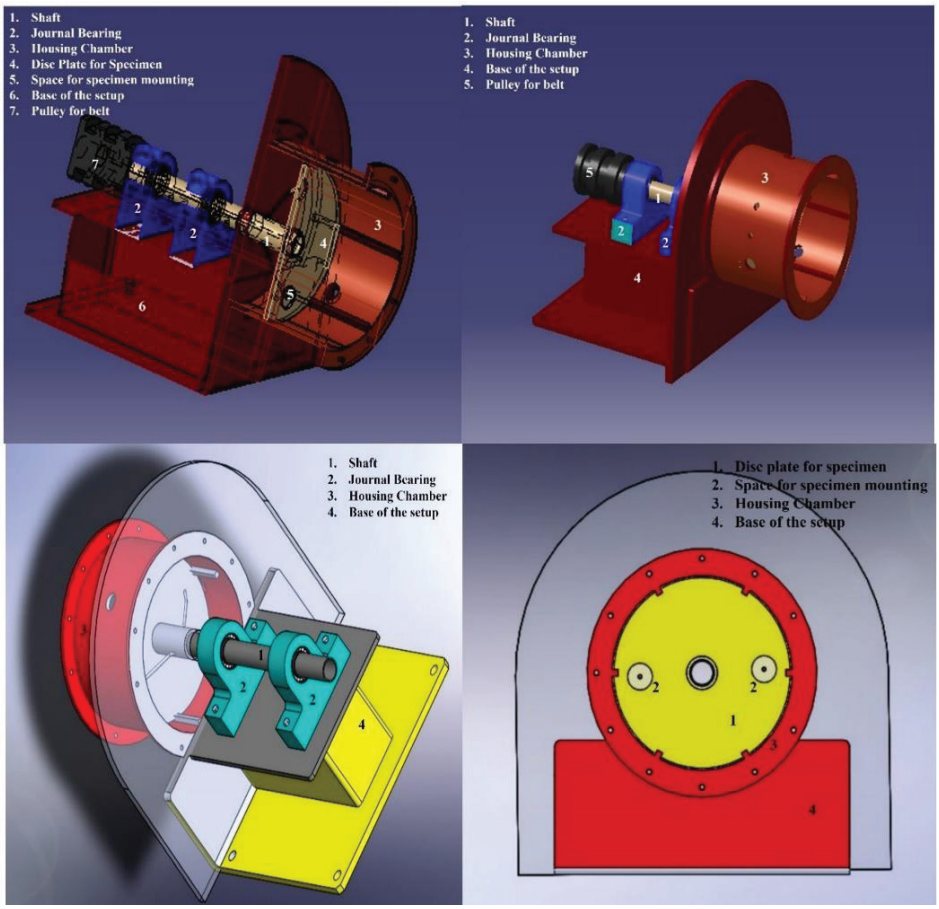
The experimental setup used for this study, the Rotating Disc Apparatus (RDA), is illustrated in Figure 3(a), with Figure 3(b) providing a 3D sketch from multiple perspectives for enhanced

Volume 10, Issue 2, December 2024 - ISSN 2356-8569
http://dx.doi.org/10.21622/RESD.2024.10.2.1054

understanding, and Figure 3(c) depicting the provisions for air injection through the setup to the test samples (either blades or guide vanes). The RDA is a rotating test setup where a fixed disc of specified dimensions revolves within silt-laden water at a predetermined speed. This system operates on the principle of mounting test samples onto a disc connected to the rotor shaft, which rotates via a pulley mechanism and high-speed motor to achieve a high relative velocity of the samples against the silt-laden water.

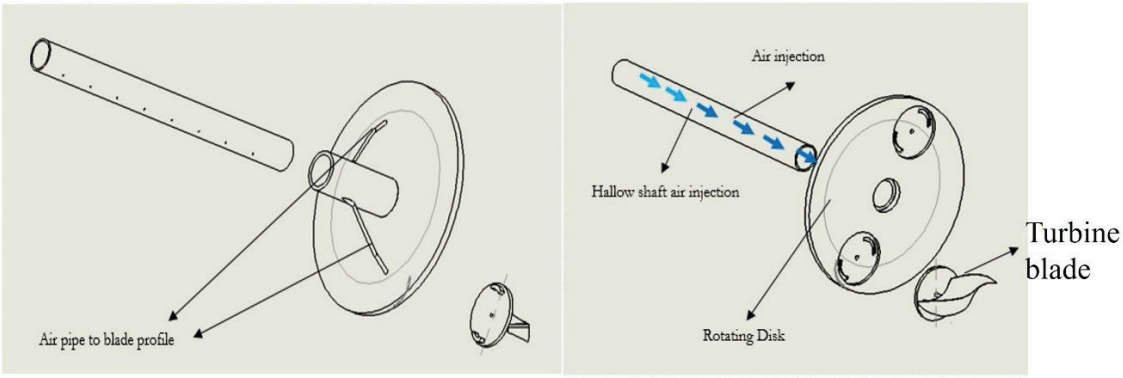


(a)



(b)

http://dx.doi.org/10.21622/RESD.2024.10.2.1054



(c)

Fig. 3. (a) Rotary Disc Apparatus (Experimental Setup) for performing erosion test (b) 3-D sketch of the experimental setup (c) Sketch showing the pathways for air injection to the samples

The sample-mounted disc in the Rotating Disc Apparatus (RDA) is enclosed within a housing filled with a sand-water mixture. Initially, the water remains stationary and is circulated from a sand-water mixing chamber to the housing via a motor pump system and two ball valves. As the samples rotate within the housing, they interact with the silt-laden water, leading to erosion on their surfaces. After a set duration, samples can be examined for erosion patterns, with material loss assessed using a precision scale. The disc and test specimens can be fabricated from softer materials or the same material as the turbine, allowing accelerated lab testing to observe sediment effects over a shorter period.

The design of the RDA components is influenced primarily by the rotational speed of the disc plate, chosen to replicate the relative velocity at the blade specimen inlet, mirroring the conditions in hydro turbine runners. A target rotational speed of 720 rpm, corresponding to approximately 15 m/s at the blade inlet, is achieved through a V-belt drive with a 1:2 pulley ratio, given the experimental motor rated speed of 1400 rpm. This speed is optimal when the water remains stationary; during testing, however, water movement along with the rotating disc reduces the relative velocity slightly below 15 m/s. The motor capacity is estimated to account for the torque needed to overcome drag forces exerted by the water on all rotating components, as well as hydraulic and mechanical system losses. These drag forces act on the disc face, the test specimen surfaces, and the cylindrical surface of the rotating disc. An 18.5 kW, three-phase, two-pole induction motor powers the disc rotation.

In this study, the accelerated experimental setup is used to analyse erosion effects on guide vanes within a silt-laden environment inside a closed chamber, simulating conditions for Francis turbines. By adjusting parameters such as shaft speed and flow discharge, the setup can replicate both partial and full load conditions. Additionally, silt concentration levels within the chamber can be varied to account for seasonal changes, enabling realistic simulations. While this study proposes an erosion mitigation technique for guide vanes, further research is needed to investigate a range of parameters, including varied shaft speeds, silt concentrations, and guide vane angles of attack under different loading conditions. These variables form the basis of future studies.

2. Guide Vane Samples and Sediment Samples

The complex processes of silt erosion are investigated by collecting sediment samples from the Maneri Bhali Hydroelectric Project. Samples are extracted from the settling basin to gain a firsthand understanding of silt behavior within the reservoir. This careful investigation involves dividing the silt into three unique sizes: 250 µm, 100 µm, and 50 µm. Such meticulous classification sets the stage for a comprehensive exploration of sediment transport mechanisms and effective management strategies, vital for ensuring the sustainable operation of hydroelectric power plants like Maneri Bhali. Models of the guide vanes used in Francis's turbines are used as specimens during the experimental procedure. Samples for the testing are used in two categories. Red oxide samples without and with an air injection facility, as shown in Figure 4 (a) and Figure 4 (b). Second are anodized samples without and with the air injection facility shown in Figure 4 (c) and Figure 4 (d), respectively.

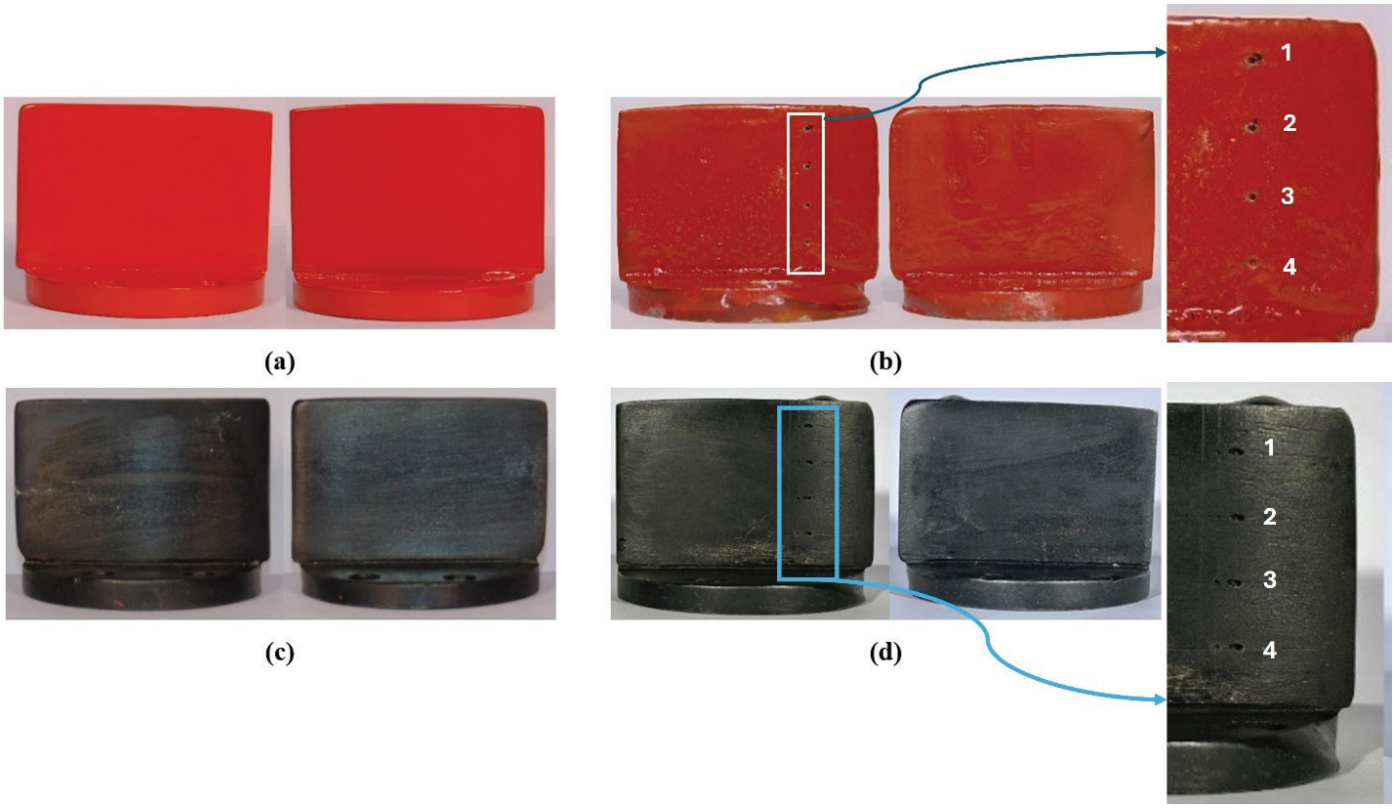


Fig. 4. Fabricated guide vane samples replicating guide vane of Francis Turbines (a) red oxide samples without air injection facility, (b) red oxide samples with air injection facility on the pressure side, (c) anodized samples without air injection facility, and (d) anodized samples with air injection facility on the pressure side

The conventional manufacturing methods used for producing guide vanes in Francis turbines were employed to replicate the specimen guide vane profiles for this study. Utilizing established techniques commonly applied in turbine production facilities, the blade shapes are machined with high precision to ensure structural accuracy. These test specimens are specifically designed to mirror the structural and functional characteristics of operational guide vanes in Francis turbines. This approach aims to provide a thorough understanding of guide vane behavior and performance under varied conditions, contributing valuable insights toward developing optimized turbine design and performance strategies.

3. Experimental Parameters

The thorough selection and adaptation of parameters are critical to the integrity and reliability of experiments. Identifying and defining these parameters is more than just a procedure; it represents a purposeful attempt to control influential variables that directly influence experimental results. The parameters generally serve in two capacities: as variables for examination and as lenses through which phenomena are observed and evaluated. The fundamental basis upon which theories for erosion tests are examined and conclusions drawn consists of parameters ranging from sediment suspension in a water mixture and air injection flow rate to sediment size and air injection hole size. To effectively imitate field conditions and create mitigation methods, a variety of criteria must be considered while designing erosion tests for guide vane samples. To get accurate and meaningful findings, the experimental setup, and its parameters, like the operational environment and measurement methods, must all be carefully considered [49], [50].

http://dx.doi.org/10.21622/RESD.2024.10.2.1054

TABLE II
DIFFERENT PARAMETERS OF THE RDA SETUP.

Sr. No.	Parameters	Value
Hydraulic and Flow Parameters		
1.	Speed of disc plate	720 rpm
2.	Angle of attack of hydrofoil	10°
3.	Capacity of the RDA casing	14 liters
Air-Injection Parameters		
4.	Means of air-injection	4 holes on the pressure side
5.	Size of holes	1 mm diameter
6.	Angle of air-injection	~50°
7.	Air flow rate	15 L/min
Geometrical and structural parameters		
8.	Diameter of disc	390 mm
9.	Guide vane profile	NACA 4412
Environmental and Material parameters		
10.	Sediment Size range	50 – 250 μm
11.	Silt Concentration	85000 ppm
12.	Operating time	400 minutes per sample
13.	Operating temperature	Ambient Temperature (about 25°C – 28°C)

C. *Error Analysis*

In the experiment conducted, a range of measurements is collected, each accompanied by specific uncertainties that could affect the overall findings. The weights of the specimens varied between 130 g and 160 g, with an average relative uncertainty of approximately 0.017%, stemming from a measurement error of ±0.0246 g. The air volume is measured at 15 L/s, yielding a relative uncertainty of about 0.0283%, which is due to a ±0.2546 L/min error in the flow meter. The recorded rotations per minute (RPM) are 720, with a relative uncertainty of 0.124% arising from an absolute error of ±0.89. Additionally, the angle of attack is set at 10 degrees, exhibiting a notable relative uncertainty of 5% attributed to a ±0.5-degree measurement error. These uncertainties underscore the potential for error in the experimental results, highlighting the necessity of precise measurements to ensure the reliability of the outcomes. Therefore, while the experiments yield valuable insights, the inherent uncertainties call for careful interpretation of the results and an awareness of their potential impact on the conclusions reached.

The analysis of material loss in the experimentation over a period of 400 minutes for each specimen produces significant findings. The cumulative material loss varied between 1.11 g and 1.55 g across the specimens. The average material loss is found to be approximately 1.346 g, indicating a general trend of material degradation among the samples. A standard deviation of 0.2021 g suggests moderate variability in material loss, reflecting some inconsistency among the specimens. This variability is further illustrated by a coefficient of variation (CV) of 15.02%, indicating that the standard deviation represents about 15% of the mean. Consequently, the reliability of the experimental results is estimated to be 84.98%, suggesting a high degree of confidence in the consistency of the observed material loss across the specimens. These figures emphasize the importance of accurate measurement and thorough analysis in understanding the behavior of materials under experimental conditions.

III. RESULTS AND DISCUSSION

This study aims to extend the operational lifespan of hydro turbines by introducing a novel approach for reducing silt erosion through the injection of a secondary fluid into existing hydro turbine arrangements. To focus on the primary objective—

Volume 10, Issue 2, December 2024 - ISSN 2356-8569
http://dx.doi.org/10.21622/RESD.2024.10.2.1054

understanding the impact of air injection on erosion—the study limited its scope to essential operational factors. The significance of this research lies in its innovative method, offering a means to prolong turbine life efficiently while preserving the material integrity of blades and other critical components. Both simulations and experimental analyses confirm that air injection onto guide vane surfaces can significantly mitigate silt erosion. The study utilizes an aerated guide vane, similar to the ventilated turbine design used in previous research [33]. Findings suggest that air injection mitigates sediment erosion through multiple mechanisms: creating a protective layer, altering flow behavior, and facilitating sediment displacement.

A. Simulations Results

This simulation study examines the erosion of guide vane caused by sediment particles present in silt-laden water streams, by performing simulations for the interaction of air-water (silt-laden water) with the surface of guide vane. and flow dynamics of a guide vane that has a profile of NACA 4412 hydrofoil, commonly used in Francis turbines. The O-Grid Hexahedral mesh element counts for cases 1, 2, and 3 are 0.949, 1.276, and 1.401 million, respectively, while the Cartesian Cut mesh counts for cases 4, 5, and 6 are 0.51, 1.04, and 1.241 million. The operating parameters are sediment levels in the water stream (*m*) of 2500 ppm and 5000 ppm, air injection velocities (*v*) ranging from 7.5 m/s to 17.5 m/s, and injection angles (*d*) of 30° and 90°. Additionally, the hydrofoil angle of attack (*a*) is considered at 10°, with a free stream velocity of 10 m/s. Erosion wear behavior, both with and without air injection, is predicted using the Euler-Euler-Lagrange model coupled with the *K*-omega SST turbulence model. Air is injected through a continuous slit located at $y = L/8$ from the leading edge, with an aspect ratio (*AR*) of 3.42. The effects after the introduction of air injection are presented in Figure 5, which shows the difference between erosion rate with and without air injection. If observed, the first impact of the silt-laden water with a guide vane shows higher readings of the erosion rate because the air envelope is not present at that place. The moment the air envelope is established, the effect of that can be observed in the fall of the values of erosion rate. The difference in the erosion rate of both cases is significant during the first half of the span because there is no separation of the silt laden fluid from the surface, later on it reduces in both the cases, even though it is very less in the air injection case.

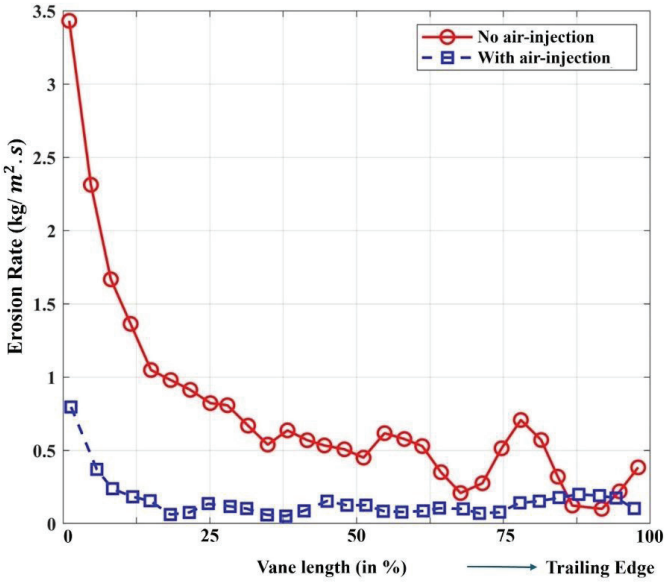


Fig. 5. Erosion rate vs sample length in no air and with air injection at $a = 10°$, $m = 2500$ ppm, $d = 90°$ and $v = 7.5$ m/s

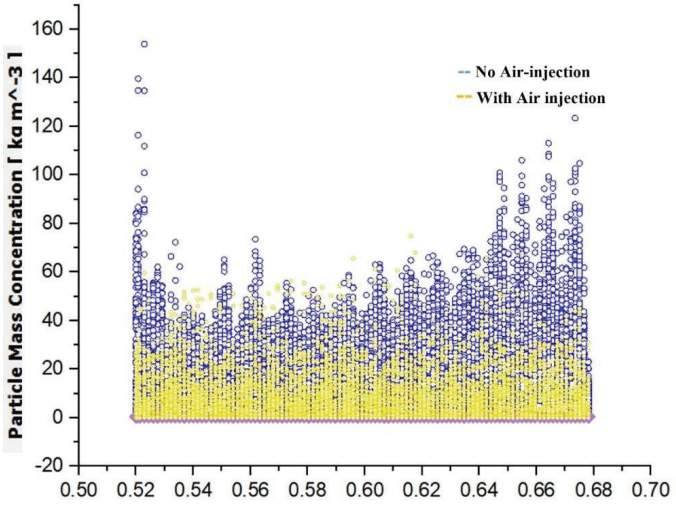


Fig. 6. Sediment particle distribution over the surface of the guide vane without and with air injection for $a = 10°$, $m = 2500$ ppm, $d = 90°$ and $v = 7.5$ m/s

The sediment particle distribution shown in Figure 6 illustrates the interaction of sediment particles along the guide vane surface, where an air envelope facilitates particle displacement through a "carried-away" effect. As a significant portion of sediment particles is removed by the airflow, it is inferred that the guide vane surface experiences reduced erosion and material loss. To investigate further, air injection velocity is increased, and the corresponding erosion rates, presented in Figure 7, demonstrate a decline in erosion as air velocity rises. Enhanced flow dynamics at higher velocities diminish the interaction between sediment particles and the vane surface, thus lowering erosion rates. However, increasing air injection velocity beyond a certain

Volume 10, Issue 2, December 2024 - ISSN 2356-8569
http://dx.doi.org/10.21622/RESD.2024.10.2.1054

threshold does not further reduce erosion; Figure 7 indicates that the optimal reduction occurs at an air injection velocity of 12.5 m/s. As air injection velocity (*v*) increases past this point, surface turbulence rises, disrupting the carried-away effect and diminishing the effectiveness of the air envelope. Although erosion remains lower than without air injection, careful consideration of higher velocities is essential to maintain the technique efficacy in mitigating silt erosion on guide vanes. Additionally, calculations suggest that velocity values are relatively similar across the mid-span, likely due to dynamic flow changes, underscoring the need for cautious application of higher velocities for optimal erosion control.

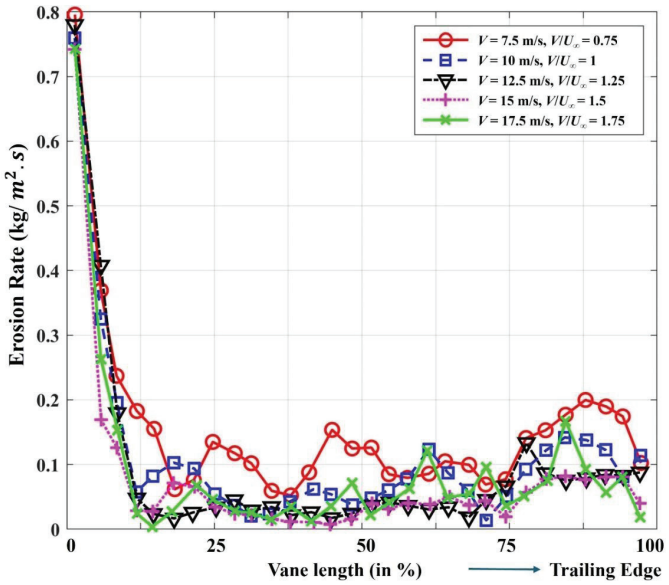


Fig. 7. Erosion rate vs guide vane length with air injection at *a* = 10°, *m* = 2500 ppm, *d* = 90° and *v* = varying from 7.5 m/s to 17.5 m/s

The CFD flow visualization shown in Figure 8 and Figure 9 demonstrate the flow of air injected over the surface of guide vane in the water stream. Figure 8 displays volume fraction of air exiting the slit from guide vane at an angle of attack of 33° inside water domain at varying air injection velocities of (a)7.5 m/s and (b)27.5 m/s. These images illustrate the complex interactions between the water and injected air, highlighting how different velocities influence the flow patterns around the vane. As the air injection rate increases, the air flow demonstrates significant changes, including alterations in turbulence levels and vortex formation. The volume fraction of air exiting the slit from the guide vane at a 10° angle of attack within the water domain is illustrated in Figure 9, showing variations at air injection velocities of 27.5 m/s, 15 m/s, and 7.5 m/s. This visualization provides crucial insights into the distribution and concentration of air-envelope over the guide vane within the fluid. The images indicate areas of high air concentration, which are often linked to regions of intense turbulence or where air is actively injected. Analyzing the volume fraction allows for a better understanding of how the air-water interaction affects the overall flow characteristics. These figures illustrate the relationship between air injection rates and flow behavior, underscoring the importance of optimizing injection parameters to achieve desired performance outcomes in fluid dynamics applications.

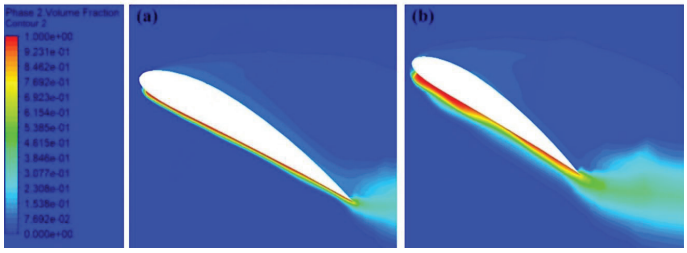


Fig. 8. Volume fraction of air exiting the slit from guide vane at a high angle of attack of 33° inside water domain at varying air injection velocities of (a) 7.5 m/s and (b) 27.5 m/s

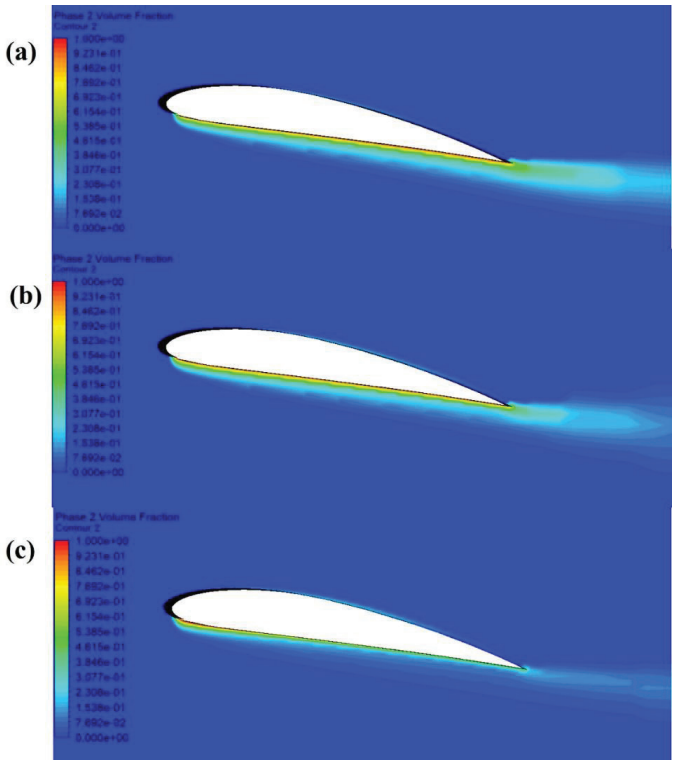


Fig. 9. Volume fraction of air exiting the slit from guide vane at an angle of attack of 10° inside water domain at varying air injection velocities of (a) 27.5 m/s, (b) 15 m/s and (c) 7.5 m/s

B. *Experimentation Results*

The experimental work results in findings that

Volume 10, Issue 2, December 2024 - ISSN 2356-8569
http://dx.doi.org/10.21622/RESD.2024.10.2.1054

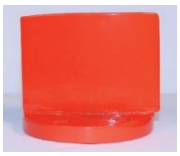
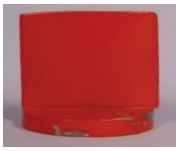
carefully fit together the pieces of simulation of air injection to mitigate silt erosion. Comprehensive analyses are performed to look at two different phenomena: the material loss observed in the specimens after each cycle, represented by graphs, and the patterns of erosion on the surfaces organized the images of the specimens after each cycle.

1. Image Visualization

This analysis provides a visual representation of the specimens, enabling clear observation and understanding of the erosion patterns. The study involves the use of two types of samples: red oxide-coated specimens for initial analysis and anodized specimens with a black coating for further evaluation. Erosion patterns are documented on both the suction and pressure sides of the guide vanes at intervals of 80 minutes, facilitating detailed, time-based analysis of the erosion progression. Table III presents the erosion patterns for red oxide samples without air injection. Following the experimental exposure, the paint coating degraded, and the underlying material exhibited visible erosion, leading to noticeable changes in surface texture and appearance. The continuous decrease in specimen weight, as shown in Figure 10, quantifies the material loss over time, with reductions recorded every 80 minutes.

Table IV demonstrates that when air injection is applied to the pressure side under identical experimental conditions, the paint removal is significantly reduced, indicating a lower rate of material erosion. A closer examination reveals that surfaces not subjected to air injections experienced a greater material loss compared to those protected by the air envelope. Due to challenges with the red oxide paint, such as uneven adhesion and peeling, anodized metal specimens are employed for more reliable results. As seen in Table V, the anodized coating provides a uniformly distributed protective layer, applied via an electrochemical process, which eliminates the issue of uneven adhesion and ensures consistent surface protection throughout the experiment. The specimens are exposed to silt-laden water, material removal occurs, leading to the onset of erosion. The progression of erosion can be observed through the images provided in Table V which depict the changes in surface condition over time. Additionally, the extent of material reduction is quantitatively illustrated in Figure 10 which tracks the loss of material throughout the experiment. These visual and quantitative data collectively demonstrate the erosion patterns and provide insight into the severity and distribution of material degradation across the specimen surface.

TABLE III
IMAGES SHOWING EROSION PATTERN FOR EVERY 80 MINUTES ON RED OXIDE SAMPLES WITHOUT AIR INJECTION SUBJECTED TO RDA CYCLES FOR 400 MINUTES.

0 minutes	80 minutes	160 minutes	240 minutes	320 minutes	400 minutes
					
					

Volume 10, Issue 2, December 2024 - ISSN 2356-8569
http://dx.doi.org/10.21622/RESD.2024.10.2.1054

TABLE IV
IMAGES SHOWING EROSION PATTERN FOR EVERY 80 MINUTES ON RED OXIDE SAMPLES WITH AIR INJECTION SUBJECTED TO RDA CYCLES FOR 400 MINUTES.

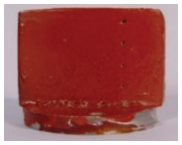
0 minutes	80 minutes	160 minutes	240 minutes	320 minutes	400 minutes
					
					

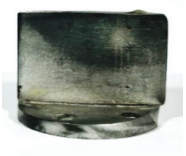
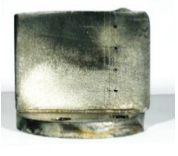
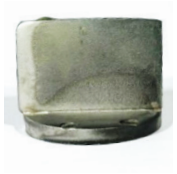
TABLE V
IMAGES SHOWING EROSION PATTERN FOR EVERY 80 MINUTES ON ANODIZED SAMPLES WITHOUT AIR-INJECTION SUBJECTED TO RDA CYCLES FOR 400 MINUTES.

0 minutes	80 minutes	160 minutes	240 minutes	320 minutes	400 minutes
					
					

Moving forward to the anodized specimen with air injection over the surface in Table VI, it shows considerable differences in the removal of black color. The areas subjected to air injection exhibited far less material removal compared to those without air injection, highlighting the effectiveness of the air envelope in preventing surface erosion. The images taken after the completion of the experimental cycles further clarify where erosion mitigation is most needed. From Table III and Table V, it is evident that the pressure side of the specimens experienced more erosion compared to the suction side. Based on this observation, air injection is applied to the pressure side to enhance protection. As demonstrated in Table IV and Table VI, the application of the air injection technique results in a noticeable reduction in material removal from the pressure side, confirming the efficacy of the air envelope in mitigating erosion in this critical area.

http://dx.doi.org/10.21622/RESD.2024.10.2.1054

TABLE VI
IMAGES SHOWING EROSION PATTERN FOR EVERY 80 MINUTES ON ANODIZED SAMPLES WITH AIR-INJECTION SUBJECTED TO RDA CYCLES FOR 400 MINUTES.

0 minutes	80 minutes	160 minutes	240 minutes	320 minutes	400 minutes
					
					

Wear refers to the gradual erosion or degradation of a metal surface caused by the abrasive impact of silt particles carried by suspended water as it interacts with the metallic samples. This inevitably leads to material loss and scratches on the surface. Figure 10 presents the material loss in various samples, highlighting the effects of air injection compared to no air injection on red oxide and anodized samples. The data demonstrate a general decrease in material loss over time across all samples, while the rate of loss is less pronounced in samples exposed to air injection.

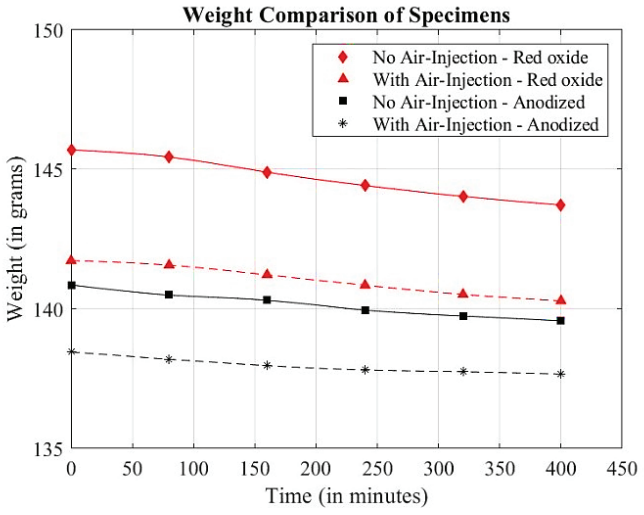


Fig. 10. Reduction in weight of samples noted after 80 minutes in one complete cycle of 400 minutes of RDA setup

For red oxide samples, material loss without air injections occurs at a rate of -0.297 grams per hour, with air injections, this rate decreases to -0.216 grams per hour, representing a reduction of approximately 27%. Similarly, anodized samples exhibit a wear rate of -0.2265 grams per hour without air injection and -0.1185 grams per hour with air injection, indicating a reduction of about 38%. Figure 11 and Figure 12 further explore this trend, detailing the wear patterns over a 400-minute operating cycle for different sample categories. Both graphs exhibit a similar trend: an initial increase in wear, followed by a gradual decrease. The initial rise is attributed to the interaction of sand particles with the finished surface, making it more susceptible to erosion and resulting in higher material loss. In the latter half of the cycle, the wear rate diminishes as surface imperfections are decreased, leaving behind a more robust, hardened surface that is better equipped to resist further erosion. Figure 13 shows the experimental results, showing both the absolute and percentage material loss for the samples under different conditions. Also, the bars from Figure 13 clearly show how moving from paint to anodized samples is better and further highlights, how the use of air injection can help in reducing the effect of silt particles in removing the material from the surface of guide vanes.

Volume 10, Issue 2, December 2024 - ISSN 2356-8569
http://dx.doi.org/10.21622/RESD.2024.10.2.1054

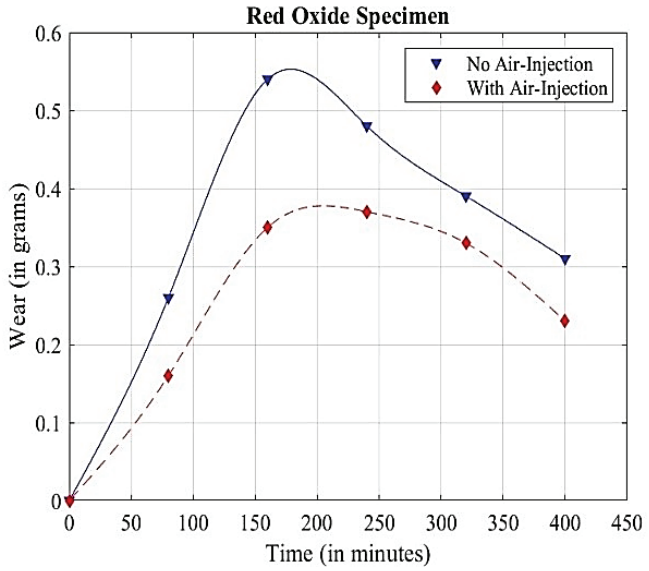


Fig. 11. Comparison of material loss in grams concerning operating time in minutes for red oxide samples with and without air injection on RDA setup

Without air injection, the red oxide samples exhibit a cumulative material loss of 1.98 grams, 1.36% of their initial weight of 145.70 grams. For the anodized samples, the cumulative material loss is 1.29 grams or about 0.91% of their initial weight of 140.86 grams over a 400-minute operating cycle. In contrast, with air injection, the red oxide samples show a cumulative material loss of 1.44 grams, around 1.01% of their initial weight of 141.73 grams. The anodized samples under air injection exhibit a cumulative material loss of 0.79 grams, or 0.57% of their initial weight of 138.46 grams, over the same period. These results indicate a reduction in material loss of approximately 27.27% for red oxide samples and 38.75% for anodized samples when air is injected. This reduction suggests that introducing an air envelope can significantly lower material loss in guide vanes, potentially extending the operational life of guide vanes and other components in hydro turbines.

For anodized samples		For Red oxide samples	
Total loss of weight without air-injection	1.29 g	Total loss of weight without air-injection	1.98 g
Total loss of weight with air-injection	0.79 g	Total loss of weight with air-injection	1.44 g
Mitigation with the introduction of air	0.50 g	Mitigation with the introduction of air	0.54 g
Percentage Mitigation	**38.75%**	Percentage Mitigation	**27.27%**

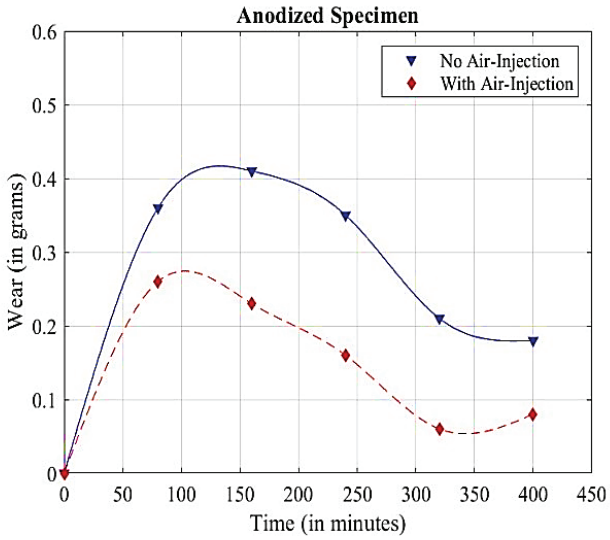


Fig. 12. Comparison of material loss in grams for operating time in minutes for anodized samples with and without air injection on RDA setup

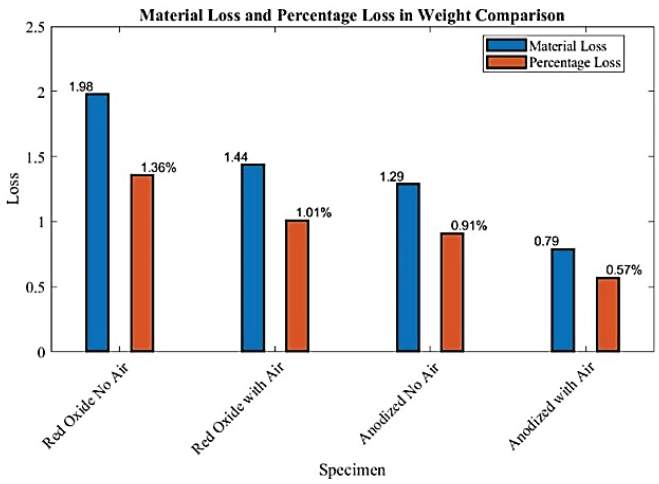


Fig. 13. Comparison chart for different specimens showing the loss in material and percentage loss in weight after using the technique for mitigation

2. Consolidated Findings: Simulation & Experiment

The integration of simulation and experimental data highlights a strong correlation and suggests that introducing this mitigation technique can minimize the major problem of hydropower plants, sediment erosion in hydro turbines. The current study focuses on the study of guide vanes used in Francis turbines, and the study allows to identify the potential sites for air injection on the surface of the guide vanes. Also, both studies suggest that a good percentage of mitigation is observed after the air injection, simply the loss of material is decreased in experimental results and the erosion rate decreases in simulation results.

a. ***Similarities and deviations:*** Both computational and experimental setups share core similarities in exploring guide vanes with a NACA 4412 profile under the impact of silt-laden water on the hydrofoil pressure side. Each setup utilizes a 10° angle of attack for the guide vanes, with ductile material properties for consistency in material response across the analyses.

However, there are significant differences between the setups. In the simulation, the interaction between the silt-laden water and the guide vane surface is quantified through slurry flow rates (e.g., 1.6 kg or 3.2 kg). Conversely, in the experimental setup, silt concentration is defined by sediment weight within a specified water volume, such as 4.25 kg of sediment in 50 liters of water (yielding a concentration of 85,000 ppm). Additional deviations arise from air flow rate measurements: in the simulation, flow rates are specified in m/s for both air and water streams, while in the experimental setup, a fixed casing rotates at 720 rpm with air injected at 15 L/s via holes supplied by a 100 psi air compressor.

The erosion rate calculation methods also vary between the two approaches. Simulation allows for erosion assessment across the entire span of the guide vane, offering particle-wise erosion data throughout. In contrast, the experimental setup quantifies erosion by weighing each specimen to determine total material loss, which further enables detailed pattern analysis of erosion that simulations cannot fully replicate. These methodological differences highlight the unique contributions of each setup to understanding and evaluating silt erosion under controlled and real-like conditions.

b. ***Validation:*** A key observation across both analyses is the observed reduction in material loss with the introduction of air injection. Experimental findings indicate a substantial reduction in erosion rates, achieving approximately 38% and 27% decreases, which align with simulation outcomes showing a material loss reduction of around 70%. The simulations enable a comprehensive assessment of material loss across the entire guide vane span, while experimental data capture the overall material loss effect along this span. Furthermore, the experimental approach, complemented by image analysis, provides a detailed view of specific erosion patterns along the vane surface.

In this study, simulation and experimental approaches are independently conducted. While simulation results support the concept of air injection over the guide vane surface, they are not intended as a direct validation of the experimental results. This distinction is due to the inherent complexity in accurately simulating real-world hydro turbine scenarios within a multi-phase environment (involving air-water-sediment-surface interactions). Replicating the intricate interactions between sediment-laden water and a guide vane surface enveloped in air under highly turbulent flow is nearly impossible with current simulation capabilities. However, simulations using well-constrained parameters allow for controlled and steady flow predictions, supporting the hypothesis that air injection can mitigate sediment erosion to some extent within these limitations.

Conversely, the experimental setup employs a scaled-down model that more closely mimics the real-world conditions of a hydro turbine. The rotating guide vanes within a sediment-laden water chamber effectively represent actual sediment erosion dynamics. In this turbulent, realistic environment, the use of a rotating disc apparatus (RDA) enables air injection on the guide vane surface, yielding positive results. The observed reduction in sediment erosion reinforces the hypothesis that air injection can mitigate silt erosion effects on guide vanes, supporting its potential application in hydroelectric turbine systems.

IV. CONCLUSION

This study highlights the effectiveness of an innovative air injection technique for mitigating

silt erosion in hydroelectric turbines—a persistent challenge in hydropower facilities. The technique is meticulously tested through both computational simulations and experimental trials using a rotating disc apparatus to evaluate erosion effects on guide vanes and runner profiles. Key findings include:

1. The pressure side of the guide vane is identified as the most erosion-prone region due to sediment impact.

2. For air injection design, a slit is simulated on the pressure side of the guide vane to create a protective air envelope around the profile. Experimentally, four 1 mm holes are used to inject air from the leading edge, optimized to the vane curvature.

3. Both computational and experimental results demonstrate a significant reduction in silt erosion upon the introduction of air.

4. Experimental findings indicate that guide vane samples coated with red oxide exhibit a 27% reduction in erosion, while anodized samples show a 38% reduction with air injection.

The consistency between computational and experimental results suggests that air injection can be feasibly scaled for practical applications, with simulation data providing reliable insights for field implementation. Although overall turbine performance remains unchanged—a point designated for future investigation—the notable reduction in erosion achieved through air injection translates into less frequent blade and vane replacements, leading to reduced maintenance time, labor, and costs. Consequently, this technique enhances turbine longevity by reducing wear on critical components. In conclusion, the protective effects of air injection contribute to improved hydropower station performance by extending the lifespan of key components and reducing operational downtime. This balance of enhanced efficiency and durability offers a net benefit, making operations more stable and cost-effective in the long term.

Acknowledgments

The authors acknowledge the support received from the Early Career Research Award, Science and Engineering Research Board, Department of Science and Technology, India under grant no. ECR/2017/002945, as well as the support received under the UPES-SEED grant program from UPES Dehradun.

Conflict of Interest

The authors declare that they have no known competing financial interests or personal relationships that could have appeared to influence the work reported in this article.

Author Contributions

Prashant Dhiman: conceptualization, methodology, data collection, formal analysis, writing and editing the original draft. Varun Pratap Singh: supervision, validation, review and editing. Ashish Karn: conceptualization, methodology, data collection, supervision, validation, writing – review and editing, manuscript revision.

References

[1] V. Singh, S. Kumar, and S. K. Mohapatra, "Modeling of Erosion Wear of Sand Water Slurry Flow through Pipe Bend using CFD," *Journal of Applied Fluid Mechanics*, vol. 12, no. 3, pp. 679–687, May 2019, doi: 10.29252/jafm.12.03.29199.

[2] U. Dorji and R. Ghomashchi, "Hydro turbine failure mechanisms: An overview," *Eng Fail Anal*, vol. 44, pp. 136–147, Sep. 2014, doi: 10.1016/j.engfailanal.2014.04.013.

[3] S. Gautam, H. P. Neopane, N. Acharya, S. Chitrakar, B. S. Thapa, and B. Zhu, "Sediment erosion in low specific speed francis turbines: A case study on effects and causes," *Wear*, vol. 442–443, p. 203152, Feb. 2020, doi: 10.1016/j.wear.2019.203152.

[4] S. Sharma and B. K. Gandhi, "Assessment of erosion wear in low specific speed Francis turbine due to particulate flow," *Advanced Powder Technology*, vol. 34, no. 9, p. 104065, Sep. 2023, doi: 10.1016/j.apt.2023.104065.

[5] S. Chitrakar, H. P. Neopane, and O. G. Dahlhaug, "A Review on Sediment Erosion Challenges in Hydraulic Turbines," in *Sedimentation Engineering*, InTech, 2018. doi: 10.5772/intechopen.70468.

[6] C. Hauer *et al.*, "State of the art, shortcomings and future challenges for a sustainable sediment management in hydropower: A review," *Renewable and Sustainable Energy Reviews*, vol. 98, pp. 40–55, Dec. 2018, doi: 10.1016/j.rser.2018.08.031.

[7] S. Mishra, S. K. Singal, and D. K. Khatod, "Design of desilting tank for small hydropower projects - a review," 2011. [Online]. Available: www.IndianJournals.com

[8] G. Singh and A. Kumar, "Performance evaluation of desilting basins of small hydropower projects," *ISH Journal of Hydraulic Engineering*, vol. 22, no. 2, pp. 135–141, May 2016, doi: 10.1080/09715010.2015.1094750.

[9] V. Almeida *et al.*, "Approach to sediment monitoring in Hydro Power Plant," *IOP Conf Ser Earth Environ Sci*, vol. 1079, no. 1, p. 012062, Sep. 2022, doi: 10.1088/1755-1315/1079/1/012062.

[10] A. Kr. Rai and A. Kumar, "Sediment monitoring for hydro-abrasive erosion : A field study from Himalayas, India," *International Journal of Fluid Machinery and Systems*, vol. 10, no. 2, pp. 146–153, Jun. 2017, doi: 10.5293/IJFMS.2017.10.2.146.

[11] M. B. Bishwakarma and H. Støle, "Real-time sediment monitoring in hydropower plants," *Journal of Hydraulic Research*, vol. 46, no. 2, pp. 282–288, Mar. 2008, doi: 10.1080/00221686.2008.9521862.

[12] M. B. Bishwakarma, "Concept Paper for a Research on Optimum Sediment Handling in Run-Of-River Hydropower Plants," in *International Conference on Small Hydropower - Hydro Sri Lanka*, 2007.

[13] G. Prashar, H. Vasudev, and L. Thakur, "Performance of different coating materials against slurry erosion failure in hydrodynamic turbines: A review," *Eng Fail Anal*, vol. 115, p. 104622, Sep. 2020, doi: 10.1016/j.engfailanal.2020.104622.

[14] D. K. Goyal, H. Singh, and H. Kumar, "Characterization and Accelerated Erosion Testing of WC-Co-Cr- and CoNiCrAlY-Coated CA6NM Turbine Steel," *Journal of Thermal Spray Technology*, vol. 28, no. 7, pp. 1363–1378, Oct. 2019, doi: 10.1007/s11666-019-00897-7.

[15] K. Goyal, "Experimental investigations of mechanical properties and slurry erosion behaviour of high velocity oxy fuel and plasma sprayed Cr 2 O 3 –50%Al 2 O 3 coatings on CA6NM turbine steel under hydro accelerated conditions," *Tribology - Materials, Surfaces & Interfaces*, vol. 12, no. 2, pp. 97–106, Apr. 2018, doi: 10.1080/17515831.2018.1452369.

[16] R.Kumar, S.Bhandari, and A.Goyal, "Synergistic effect of Al 2 O 3 /TiO 2 reinforcements on slurry erosion performance of nickel-based composite coatings," *Proceedings of the Institution of Mechanical Engineers, Part J: Journal of Engineering Tribology*, vol. 232, no. 8, pp. 974–986, Aug. 2018, doi: 10.1177/1350650117736487.

[17] K. R.K., K. M., S. S., and A. K. S., "A pragmatic approach and quantitative assessment of silt erosion characteristics of HVOF and HVAF processed WC-CoCr coatings and 16Cr5Ni steel for hydro turbine applications," *Mater Des*, vol. 132, pp. 79–95, Oct. 2017, doi: 10.1016/j.matdes.2017.06.046.

[18] V. Sharma, M. Kaur, and S. Bhandari, "Slurry erosion performance study of high velocity flame sprayed Ni–Al 2 O 3 coating under hydro accelerated conditions," *Mater Res Express*, vol. 6, no. 7, p. 076436, Apr. 2019, doi: 10.1088/2053-1591/ab1927.

[19] V. Sharma, M. Kaur, and S. Bhandari, "Development and Characterization of High-Velocity Flame Sprayed Ni/TiO2/Al2O3 Coatings on Hydro Turbine Steel," *Journal of Thermal Spray Technology*, vol. 28, no. 7, pp. 1379–1401, Oct. 2019, doi: 10.1007/s11666-019-00918-5.

[20] B. Singh and S. Zafar, "Effect of microwave exposure time on microstructure and slurry erosion behavior of Ni + 20% Cr7C3 composite clads," *Wear*, vol. 426–427, pp. 491–500, Apr. 2019, doi: 10.1016/j.wear.2018.12.016.

[21] D. K. Goyal, H. Singh, H. Kumar, and V. Sahni, "Slurry Erosive Wear Evaluation of HVOF-Spray Cr2O3 Coating on Some Turbine Steels," *Journal of Thermal Spray Technology*, vol. 21, no. 5, pp. 838–851, Sep. 2012, doi: 10.1007/s11666-012-9795-5.

[22] H. S. Grewal, H. S. Arora, A. Agrawal, H. Singh, and S. Mukherjee, "Slurry Erosion of Thermal Spray Coatings: Effect of Sand Concentration," *Procedia Eng*, vol. 68, pp. 484–490, 2013, doi: 10.1016/j.proeng.2013.12.210.

[23] H. S. Grewal, H. S. Arora, H. Singh, and A. Agrawal, "Surface modification of hydroturbine steel using friction stir processing," *Appl Surf Sci*, vol. 268, pp. 547–555, Mar. 2013, doi: 10.1016/j.apsusc.2013.01.006.

[24] S. A. Romo, J. F. Santa, J. E. Giraldo, and A. Toro, "Cavitation and high-velocity slurry erosion resistance of welded Stellite 6 alloy," *Tribol Int*, vol. 47, pp. 16–24, Mar. 2012, doi: 10.1016/j.triboint.2011.10.003.

[25] J. F. Santa, L. A. Espitia, J. A. Blanco, S. A. Romo, and A. Toro, "Slurry and cavitation erosion resistance of thermal spray coatings," *Wear*, vol. 267, no. 1–4, pp. 160–167, Jun. 2009, doi: 10.1016/j.wear.2009.01.018.

[26] M. K. Padhy and R. P. Saini, "A review on silt erosion in hydro turbines," *Renewable and Sustainable Energy Reviews*, vol. 12, no. 7, pp. 1974–1987, Sep. 2008, doi: 10.1016/j.rser.2007.01.025.

[27] A. Karn *et al.*, "Bubble size characteristics in the wake of ventilated hydrofoils with two aeration configurations," *International Journal of Fluid Machinery and Systems*, vol. 8, no. 2, pp. 73–84, Jun. 2015, doi: 10.5293/IJFMS.2015.8.2.073.

[28] A. Karn, C. Ellis, J. Hong, and R. E. A. Arndt, "Investigations into the turbulent bubbly wake of a ventilated hydrofoil: Moving toward improved turbine aeration techniques," *Exp Therm Fluid Sci*, vol. 64, pp. 186–195, Jun. 2015, doi: 10.1016/j.expthermflusci.2014.12.011.

[29] A. Karn, C. Ellis, R. Arndt, and J. Hong, "An integrative image measurement technique for dense bubbly flows with a wide size distribution," *Chem Eng Sci*, vol. 122, pp. 240–249, Jan. 2015, doi: 10.1016/j.ces.2014.09.036.

[30] A. Karn, G. M. Monson, C. R. Ellis, J. Hong, R. E. A. Arndt, and J. S. Gulliver, "Mass transfer studies across ventilated hydrofoils: A step towards hydroturbine aeration," *Int J Heat Mass Transf*, vol. 87, pp. 512–520, Aug. 2015, doi: 10.1016/j.ijheatmasstransfer.2015.04.021.

[31] Z. Chen and Y.-D. Choi, "Influence of air supply on the performance and internal flow characteristics of a cross flow turbine," *Renew Energy*, vol. 79, pp. 103–110, Jul. 2015, doi: 10.1016/j.renene.2014.08.024.

[32] K. Kumar and R. P. Saini, "A review on operation and maintenance of hydropower plants," *Sustainable Energy Technologies and Assessments*, vol. 49, p. 101704, Feb. 2022, doi: 10.1016/j.seta.2021.101704.

[33] R. E. A. Arndt, C. R. Ellis, and S. Paul, "Preliminary investigation of the use of air injection to mitigate cavitation erosion," in *American Society of Mechanical Engineers, Fluids Engineering Division (Publication) FED*, 1993.

[34] R. E. A. Arndt, C. R. Ellis, and S. Paul, "Preliminary Investigation of the Use of Air Injection to Mitigate Cavitation Erosion," *J Fluids Eng*, vol. 117, no. 3, pp. 498–504, Sep. 1995, doi: 10.1115/1.2817290.

[35] A. Karn, S. Shao, R. E. A. Arndt, and J. Hong, "Bubble coalescence and breakup in turbulent bubbly wake of a ventilated hydrofoil," *Exp Therm Fluid Sci*, vol. 70, pp. 397–407, Jan. 2016, doi: 10.1016/j.expthermflusci.2015.10.003.

[36] P. Dhiman, A. Bhat, and A. Karn, "The Efficacy of Air Injection in Mitigating Silt Erosion on Hydroturbine Blades: A Computational Study," 2024, pp. 437–444. doi: 10.1007/978-981-99-6616-5_49.

[37] A. Karn, A. Bhat, and P. Dhiman, "Multipahse flow simulations to explore novel technique of air injection to mitigate silt erosion in hydro turbines," *Journal of Applied Fluid Mechanics*, 2025.

[38] S. Aryal, S. Chitrakar, R. Shrestha, and A. kumar Jha, "Credibility of Rotating Disc Apparatus for investigating sediment erosion in guide vanes of Francis turbines," *IOP Conf Ser Earth Environ Sci*, vol. 1037, no. 1, p. 012034, Jun. 2022, doi: 10.1088/1755-1315/1037/1/012034.

[39] R. Silva, C. Cotas, F. A. P. Garcia, P. M. Faia, and M. G. Rasteiro, "Particle Distribution Studies in Highly Concentrated Solid-liquid Flows in Pipe Using the Mixture Model," *Procedia Eng*, vol. 102, pp. 1016–1025, 2015, doi: 10.1016/j.proeng.2015.01.224.

[40] Y. Zhang, E. P. Reuterfors, B. S. McLaury, S. A. Shirazi, and E. F. Rybicki, "Comparison of computed and measured particle velocities and erosion in water and air flows," *Wear*, vol. 263, no. 1–6, pp. 330–338, Sep. 2007, doi: 10.1016/j.wear.2006.12.048.

[41] R. E. Vieira, A. Mansouri, B. S. McLaury, and S. A. Shirazi, "Experimental and computational study of erosion in elbows due to sand particles in air flow," *Powder Technol*, vol. 288, pp. 339–353, Jan. 2016, doi: 10.1016/j.powtec.2015.11.028.

[42] A. Mansouri, H. Arabnejad, S. A. Shirazi, and B. S. McLaury, "A combined CFD/experimental methodology for erosion prediction," *Wear*, vol. 332–333, pp. 1090–1097, May 2015, doi: 10.1016/j.wear.2014.11.025.

[43] C. Bogey, "Grid sensitivity of flow field and noise of high-Reynolds-number jets computed by large-eddy simulation," *Int J Aeroacoust*, vol. 17, no. 4–5, pp. 399–424, Jul. 2018, doi: 10.1177/1475472X18778287.

[44] R. Koomullil, B. Soni, and R. Singh, "A comprehensive generalized mesh system for CFD applications," *Math Comput Simul*, vol. 78, no. 5–6, pp. 605–617, Sep. 2008, doi: 10.1016/j.matcom.2008.04.005.

[45] I. SADREHAGHIGHI, R. SMITH, and S. TIWARI, "An analytical approach to grid sensitivity analysis," in *30th Aerospace Sciences Meeting and Exhibit*, Reston, Virigina: American Institute of Aeronautics and Astronautics, Jan. 1992. doi: 10.2514/6.1992-660.

[46] D. Felix, I. Albayrak, and R. M. Boes, "Continuous measurement of suspended sediment concentration: Discussion of four techniques," *Measurement*, vol. 89, pp. 44–47, Jul. 2016, doi: 10.1016/j.measurement.2016.03.066.

[47] W. Tsai, J. A. C. Humphrey, I. Cornet, and A. V. Levy, "Experimental measurement of accelerated erosion in a slurry pot tester," *Wear*, vol. 68, no. 3, pp. 289–303, May 1981, doi: 10.1016/0043-1648(81)90178-2.

[48] A. Elkholy, "Prediction of abrasion wear for slurry pump materials," *Wear*, vol. 84, no. 1, pp. 39–49, Jan. 1983, doi: 10.1016/0043-1648(83)90117-5.

[49] A. Kapali, H. P. Neopane, S. Chitrakar, and O. Shrestha, "Design and development of non-recirculating type erosion test setup for hydraulic turbines," *IOP Conf Ser Earth Environ Sci*, vol. 1079, no. 1, p. 012013, Sep. 2022, doi: 10.1088/1755-1315/1079/1/012013.

[50] R. Thakur*, S. Kumar, K. Kashyap, A. Sharma, and S. Aggarwal, "Selection of Erosive Wear Rate Parameters of Pelton Turbine Buckets using PSI and TOPSIS Techniques," *International Journal of Innovative Technology and Exploring Engineering*, vol. 9, no. 1, pp. 2418–2428, Nov. 2019, doi: 10.35940/ijitee.A4408.119119.